



This item was submitted to Loughborough's Institutional Repository (<https://dspace.lboro.ac.uk/>) by the author and is made available under the following Creative Commons Licence conditions.



CC creative commons
COMMONS DEED

Attribution-NonCommercial-NoDerivs 2.5

You are free:

- to copy, distribute, display, and perform the work

Under the following conditions:

BY: **Attribution.** You must attribute the work in the manner specified by the author or licensor.

Noncommercial. You may not use this work for commercial purposes.

No Derivative Works. You may not alter, transform, or build upon this work.

- For any reuse or distribution, you must make clear to others the license terms of this work.
- Any of these conditions can be waived if you get permission from the copyright holder.

Your fair use and other rights are in no way affected by the above.

This is a human-readable summary of the [Legal Code \(the full license\)](#).

[Disclaimer](#) 

For the full text of this licence, please go to:
<http://creativecommons.org/licenses/by-nc-nd/2.5/>

Kinematics estimation of straddled movements on high bar from a limited number of skin markers using a chain model

Mickaël Begon¹, Pierre-Brice Wieber², Maurice Raymond Yeadon¹

¹School of Sport and Exercise Sciences, Loughborough University, Loughborough Leics. LE11 3TU, United Kingdom

²INRIA Rhône-Alpes, Inovallée 655 avenue de l'Europe, Montbonnot 38 334 Saint Ismier Cedex France

Accepted 16th October 2007

Abstract

To reduce the effects of skin movement artefacts and apparent joint dislocations in the kinematics of whole body movement derived from marker locations, global optimisation procedures with a chain model have been developed. These procedures can also be used to reduce the number of markers when self-occlusions are hard to avoid. This paper assesses the kinematics precision of three marker sets: 16, 11 and 7 markers, for movements on high bar with straddled piked posture. A three-dimensional person-specific chain model was defined with 9 parameters and 12 degrees of freedom and an iterative procedure optimised the gymnast posture for each frame of the three marker sets. The time histories of joint angles obtained from the reduced marker sets were compared with those from the 16 marker set by means of a root mean square difference measure. Occlusions of medial markers fixed on the lower limb occurred when the legs were together and the pelvis markers disappeared primarily during the piked posture. Despite these occlusions, reconstruction was possible with 16, 11 and 7 markers. The time histories of joint angles were similar; the main differences were for the thigh mediolateral rotation and the knee flexion because the knee was close to full extension. When five markers were removed, the average angles difference was about 3°. This difference increased to 9° for the seven marker set. It is concluded that kinematics of sports movement can be reconstructed using a chain model and a global optimisation procedure for a reduced number of markers.

1 Introduction

In sports biomechanics, as in clinical gait analysis, optoelectronic motion capture systems based on passive markers are widely used to recover human movement descriptors. The poses (position and orientation) of the body segments are determined from skin-mounted markers before their kinematics and kinetics are calculated. In the direct approach (Kadaba et al., 1990), at least three markers per segment are needed for the definition of a segment-embedded reference frame which represents the pose of the segment. This approach has numerous limitations associated with the number of markers and the use of a rigid segment representation. Moreover the kinematics remains inaccurate because no compensation is made for the skin movement artefacts (Reinschmidt et al., 1997a).

The kinematics accuracy can be improved by increasing the number of markers per segment (Challis, 1995). The calculation of the rotation matrices from five markers seems to be a good compromise to limit the damaging effect of skin movement artefacts. In clinical analysis, there exist marker sets (Davis et al., 1991) which are used to minimize the number of markers. Joint centres are defined from static data acquisitions or from measurements on the participant. These marker sets are based on assumptions which allow the medial markers to be removed during walking trials. For these marker sets, the joint centre location is estimated with a predictive approach based on anthropometrical measurement or the midpoint of two markers.

Human kinetics calculation is often based on multibody dynamics assuming pin joints without translation. However with at least three markers, each body segment can be considered independently of the proximal one and will have three degrees of freedom (*DoF*) in rotation and three *DoF* in translation. Kinematic and kinetic parameters are calculated from non-rigid arrays of markers and procedures have been developed to limit the array deformation (Chèze et al., 1995; Spoor and Veldpaus, 1980). In these

formulations, each segment is treated independently without guaranteeing a constant segment length. To reduce skin movement artefacts and apparent joint dislocations, Lu and O'Connor (1999) proposed a global optimisation procedure with a chain model. This method has been applied to computer simulated movements of the lower limbs (Lu and O'Connor, 1999) and the upper limbs (Roux et al., 2002). Other chain models associated with optimisation procedures have been used to analyse gait (Charlton et al., 2004; Reinbolt et al., 2005). In Reinbolt et al. (2005) the determination of the kinematics was based on a two-level optimisation and required three markers per segment. Performance measures of this algorithm were estimated for 12-*DoF* synthetic motions.

In contrast with gait analysis, no standard marker set can be used satisfactorily for data collection in sport. Each movement has its own segment deformations arising from muscle contractions and joint motions together with its own self-occlusions that require a specific marker set. Additionally, the use of three or more markers per segment is impractical for whole body sports movements because of increased marker occlusion, increased soft tissue movement and increased marker detachment during dynamic movements.

Usually the joints are modelled as ball-and-socket (*e.g.* hip joint or glenohumeral joint) or as hinge joints (*e.g.* knee). If the joint centre location is known then there is some redundancy in using three markers since two will suffice for a three *DoF* joint and one marker will suffice for a single *DoF* joint. The purpose of this study was to determine the kinematics of a movement from a limited number of markers and the definition of a person-specific chain model.

2 Methods

A 9-parameter, 3-dimensional, 12-*DoF* model was used to describe the kinematics of circling movements with a piked and straddled posture on the high bar in gymnastics. This chain model was designed for this specific application, but the method is general enough to allow any model to be defined. Twenty-two technical and anatomical reflective markers were used to define the chain model. Kinematics was calculated from 16, 11 and 7 markers and then the three sets were compared to quantify the effect of the marker number. The model implementation and the kinematics optimisation from real data were performed using the *HuMANs* toolbox under Scilab (Wieber et al., 2006).

The body was considered as an articulated system composed of rigid bodies corresponding to the following segments: upper limbs, scapular girdle, torso-head, pelvis, right thigh, left thigh, right shank-foot and left shank-foot. The kinematics of the left and right lower-limbs was viewed as being symmetrical. Six parameters (p_i) and 12 *DoF* (q_i) described the chain model (Fig. 1). Flexion, abduction and lateral rotation were defined to be positive and the angle sequence was flexion-extension, abduction-adduction and mediolateral rotation.

The participant, a member of the Great Britain Men's Senior Gymnastics Squad (17 years, 61.6 kg, 1.705 m), gave informed consent to perform a number of straddled stalders and endos on the high bar (Fig. 2) changing technique and velocity from trial to trial. Ten successful trials of each of the two circling movements were selected for analysis.

All trials were captured using 18 Vicon cameras operating at 100 Hz and positioned on a hemisphere on the left side of the subject. A volume centred on the high bar spanning $3\text{ m} \times 5\text{ m} \times 5\text{ m}$ was wand calibrated. Twenty-one spherical markers of 25 mm diameter were attached to the trunk and the left upper and lower limbs: lateral and medial malleolus ($T_{1,2}$), tibia (T_3), lateral and medial knee ($T_{4,5}$), lateral side of the mid-thigh (T_6), left and right anterior superior iliac spines ($T_{7,8}$), left and right posterior superior iliac spines ($T_{9,10}$), xyphoid (T_{11}), manubrium (T_{12}), first thoracic vertebra (T_{13}), a rigid tripod fixed on the acromion (T_{14-16}), under the deltoid (T_{17}), medial side of the elbow (T_{18}), olecranon (T_{19}), and lateral and medial wrist ($T_{20,21}$). One additional marker was placed at the middle of the bar (T_{22}) between the hands. Markers T_{14-16} were removed before the data collection for the circling movements.

The dimensions of the model and the marker locations with respect to (*wrt*) the local segment reference frame had to be determined accurately. These required the determination of the centre of rotation (CoR) location and the definition of the local frame associated with each body segment. Predictive and functional approaches were used involving static and dynamic data acquisition. The glenohumeral and hip CoR (modelled as ball and socket) were located with the symmetrical CoR estimation method (Ehrig et al., 2006) in line with the recommendation of Begon et al. (2007) and Monnet et al. (in press) from markers T_{14-19} and T_{3-10} respectively. The pelvis local frame was calculated from four markers (T_{7-10})

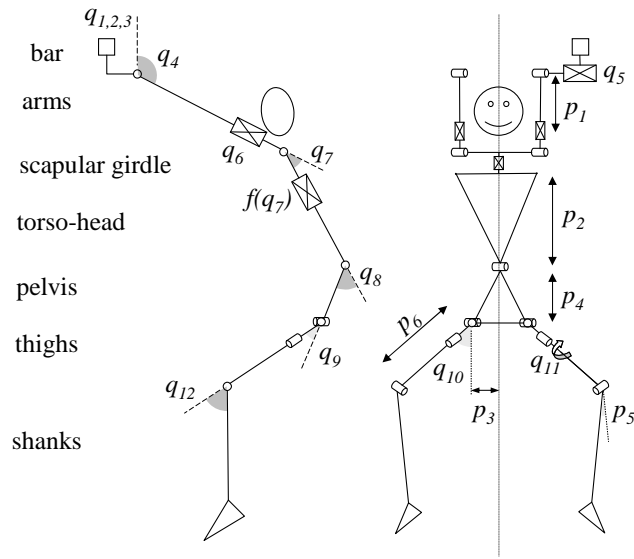


Figure 1: Model definition with the degrees of freedom and the parameters for the straddled circling movements on high bar. Degrees of freedom: q_{1-3} translation of the bar, q_4 arm rotation, q_5 arm translation, q_6 arm lengthening, q_7 shoulder flexion, q_8 , spinal flexion, q_9 thigh flexion, q_{10} thigh abduction, q_{11} thigh lateral rotation and q_{12} knee flexion. Parameters: p_1 arm length, p_2 torso length, p_3 half-width of the pelvis, p_4 pelvis height, p_5 knee adduction and p_6 thigh length.

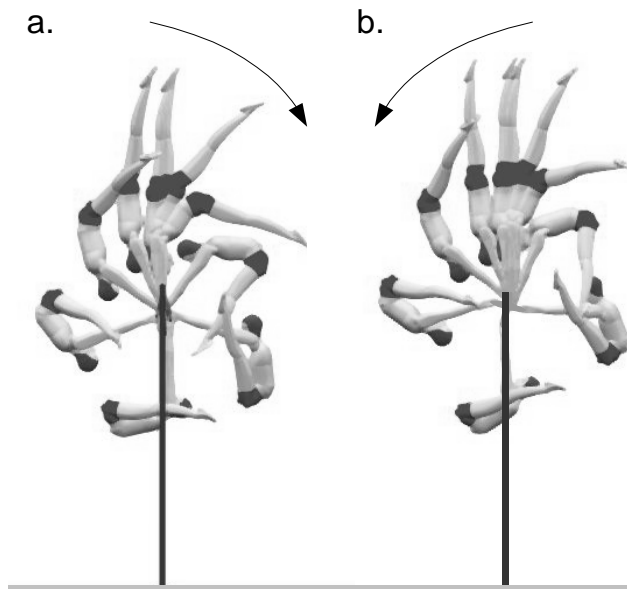


Figure 2: Straddled stalder (a) and endo (b) on high bar.

using an optimisation procedure (Challis, 1995). The elbow, wrist, knee, and ankle CoR (modelled as hinge joints) were determined as the midpoint of lateral and medial markers. The torso CoR relative to the pelvis was defined according to the anthropometrical model of Yeadon (1990). Then the parameters were personalised for the gymnast from the CoR locations during a static trial in anatomical posture. Arm flexion causes elevation of the glenohumeral joint due to rotation about the sternoclavicular joint. An initial position of the glenohumeral joint *wrt* the torso frame was determined using the static trial data. From a trial with arm flexion-extension motion, the scapular girdle elevation was modelled as a linear function f of the arm flexion q_7 . The location of each marker was expressed in the local frame of the corresponding body segment and these locations were introduced into the model.

From the data acquisition of stalders and endos on high bar, the generalized coordinates (q_{1-12}) were optimised for each frame. The resulting global optimisation was a non-linear programming problem so it had to be evaluated numerically using iterative optimisation methods (a Newton-Gauss non-linear least square algorithm). The reconstruction process was static; each posture was determined independently from the one before. Ideally we would like to obtain the generalized position vector $\mathbf{q} = q_{1-12}$ such that: $Tags(\mathbf{q}) = \mathbf{T}$, where $Tags(\mathbf{q})$ is the forward kinematics function of the chain model and $\mathbf{T} = T_{1-13,17-22}$ is the matrix of the observed marker positions. Based on the Jacobian of the $Tags$ ($\partial T_i / \partial q_j$), the generalized co-ordinates were iteratively optimised in order to minimize $\|Tags(\mathbf{q}) - \mathbf{T}\|^2$.

Three sets of kinematics were calculated using the chain model with, for each segment, three markers (Kin_{16}): $T_{1-7,9-13,19-22}$, two markers (Kin_{11}): $T_{1,3,4,6,7,9,11,13,19,21,22}$ or only one marker except for the pelvis with two markers (Kin_7): $T_{1,4,7,9,11,19,22}$. Kin_{16} was considered as the reference marker set. As skin deformation occurs in areas closer to the joints (Cappozzo et al., 1996), the markers used for Kin_{11} and Kin_7 were chosen far from joints with large ranges of motion (shoulder, hip, back).

For each set of kinematics, the global error of reconstruction was defined by:

$$\frac{1}{M} \sum_{M=1}^M \frac{1}{F_m} \sum_{f=1}^{F_m} \sqrt{\frac{1}{3 \times N_{f,m} - 12} \sum_{n=1}^{N_{f,m}} \|Tags(\mathbf{q}) - \mathbf{T}\|^2},$$

where M is the number of trials, F_m is the number of frames for trial m and $N_{f,m}$ is the numbers of visible markers for frame f in trial m . The time histories of each generalized co-ordinate were compared by means of a root mean square difference (RMSD). RMSD of Kin_7 and Kin_{11} relative to Kin_{16} were compared by means of a paired t -test ($p < 0.05$).

3 Results

The reconstructions were processed in 57 ± 14 ms, 44 ± 9 ms and 131 ± 31 ms for one frame of data and the global errors of reconstruction were 26.9 ± 3.0 mm, 26.7 ± 3.4 mm and 31.4 ± 2.5 mm for Kin_{16} , Kin_{11} and Kin_7 respectively. Whatever the trial, this error estimate increased from Kin_{11} to Kin_7 . The marker occlusions varied from 0% to 65% of the total number of frames depending on the marker (Table 1). There were no occlusions for the markers $T_{1,3,4,6,9,11,18,19,21,22}$. The occlusion number of the other markers could reach half the frames (T_8) or exceed it ($T_{5,10}$). The occlusions of the markers fixed on the medial side of the lower left limb occurred when the legs were together, and the pelvis markers disappeared mainly during the piked posture. For Kin_7 the markers were reconstructed in all the frames for the 20 movements except for the left anterior superior iliac spine T_7 which had 22% occlusions ($\pm 6\%$). Among the markers used for Kin_{11} , the first thoracic vertebra marker T_{13} also had a few occlusions ($4 \pm 7\%$).

In general, the joint angles calculated from the three marker sets were similar (Fig. 3). The main differences were for the thigh mediolateral rotation (q_{11}) and the knee flexion (q_{12}). The RMSD of the joint angles over the 20 circling movements ranged from 1° to 39° (Table 2). The RMSD of the arm rotation about the bar q_4 for Kin_{11} and Kin_7 relative to Kin_{16} never exceeded 2.2° . For Kin_{11} the maximum RMSD of the angles was less than 13.0° and the average RMSD was about 3.7° . The maximum values were found for the thigh mediolateral rotation (q_{11}). For Kin_7 this angle was imprecise with an average RMSD of 39° for a 56° range of motion. The other angles had an average difference of 4° . The RMSD of the prismatic joints ($q_{5,6}$) remained less than 6 mm for Kin_{11} and were in the order of a centimetre for Kin_7 .

Table 1: Marker occlusions during the circling movements

		mean	SD
Shank	T_1	0	(0)
	T_2	9	(17)
	T_3	0	(0)
Thigh	T_4	0	(0)
	T_5	65	(11)
	T_6	0	(0)
Pelvis	T_7	22	(6)
	T_8	42	(8)
	T_9	0	(0)
Torso	T_{10}	56	(14)
	T_{11}	0	(0)
	T_{12}	1	(2)
Upper-limb	T_{13}	4	(7)
	T_{17}	6	(6)
	T_{18}	0	(0)
	T_{19}	0	(0)
	T_{20}	6	(6)
	T_{21}	0	(0)
Bar	T_{22}	0	(0)

Note: the average values and the standard deviations are expressed as a percentage of the number of frames.

Table 2: Root mean square difference for each global co-ordinate of Kin_{11} and Kin_7 relative to Kin_{16} , with notation $Kin_{11/16}$, $Kin_{7/16}$ respectively

	q_i	Unit	$Kin_{11/16}$	$Kin_{7/16}$	p	RoM
Arm Rotation	4	[°]	0.5 ± 0.1	1.3 ± 0.3	< 0.001	457 ± 154
Arm Translation	5	[mm]	4.1 ± 1.2	4.4 ± 1.9	0.49	33 ± 7
Arm Lengthening	6	[mm]	3.3 ± 0.6	12.3 ± 2.6	< 0.001	158 ± 18
Shoulder Flexion	7	[°]	2.1 ± 0.5	4.9 ± 1.0	< 0.001	64 ± 11
Spinal Flexion	8	[°]	3.5 ± 0.9	4.4 ± 1.2	< 0.001	87 ± 12
Thigh Flexion	9	[°]	2.0 ± 0.5	6.0 ± 1.7	< 0.001	131 ± 9
Thigh Abduction	10	[°]	0.6 ± 0.1	2.6 ± 0.8	< 0.001	53 ± 7
Thigh torsion	11	[°]	10.0 ± 1.2	38.9 ± 7	< 0.001	56 ± 5
Knee Flexion	12	[°]	2.6 ± 0.7	4.8 ± 2.1	< 0.001	20 ± 8

Note: the fifth column is the p -value of the paired t -test between $Kin_{11/16}$ and $Kin_{7/16}$. The last column is the range of motion (RoM) calculated with Kin_{16} .

Only the RMSD of q_5 (translation of the arm *wrt* the bar) did not change significantly ($p = 0.49$) with the number of markers (Table 2). The other co-ordinates differed significantly ($p < 0.001$); the RMSD values increased systematically with a reduction in marker number. On average, the RMSD values for Kin_7 and Kin_{11} differed by less than 4° for $q_{4,7,8,9,10,12}$ and by 9 mm for q_6 . The main change was the thigh mediolateral rotation where the RMSD increased from 10° to 39° when $T_{3,6}$ were removed in the change from Kin_{11} to Kin_7 .

4 Discussion

The purpose of this study was (*i*) to apply a global optimisation on a fast movement with large range of motion and (*ii*) to reduce the number of markers for the kinematics reconstruction. A 9-parameter,

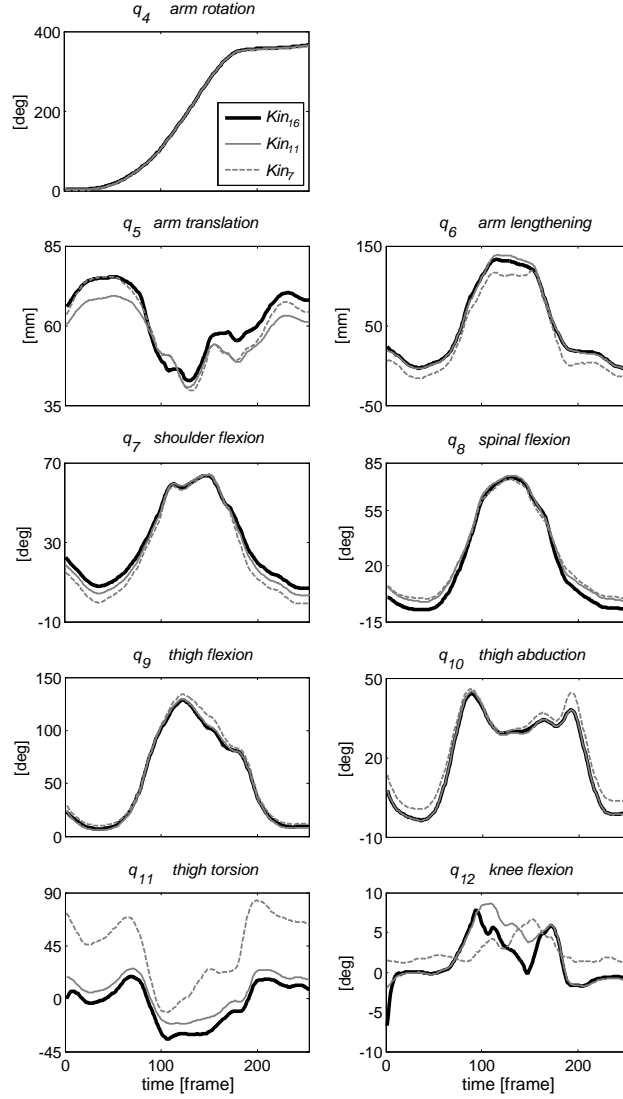


Figure 3: Time histories of the generalized co-ordinates for an endo calculated with 16, 11 and 7 markers.

3-dimensional, 12-*DoF* chain model was shown to be suitable for modelling straddled movements on high bar and the kinematics reconstruction was precise with 11 markers or 7 markers except for the thigh mediolateral rotation.

The proposed model seems to be a reasonable compromise between accuracy and simplicity of gymnast description for movements on high bar. The model was defined after observation, analyses and knowledge about circling movements on high bar (Hiley and Yeadon, 2003, 2005). On one hand, the kinematics is constrained by the gymnastics rules (*i.e.* symmetrical movements, full extension of some joints); on the other hand the kinematics of the shoulder is complex and the body length increases due to the high internal forces associated with the centripetal accelerations.

For simplicity of the model, the foot and head segments were considered to be fixed *wrt* the shank and the torso respectively and the elbow was kept fully extended. In gymnastics, the foot has to be aligned with the shank and the lower-arm aligned with the upper-arm. The small amplitude of rotation of these joints could have only a small effect on the dynamics. Simple ball and socket or hinge joints do not model the real musculoskeletal system accurately (Lu and O'Connor, 1999); however joint models that are more anatomical can be defined. The previous gymnast models for high bar movements (Hiley and Yeadon, 2003, 2005) have been improved by introducing an extra *DoF* between the torso and the pelvis and by a personalised behaviour of the scapular girdle elevation as a function of arm flexion (q_7).

The elevation of the scapular girdle could not be estimated by the global optimisation procedure because it would cause a singularity with q_6 (arm lengthening) when $q_7 = 0 \pm \pi$ (shoulder flexion), *i.e.* if arm and trunk were aligned. The joint location in the back was determined from observation of the whole spine flexion and according to the anthropometrical model of Yeadon (1990). This chain model defined for mechanical analysis and optimisation of circling movement with piked straddled postures has to be associated with an anthropometrical model to calculate the kinetics.

The main experimental problem of straddled movements on high bar was the marker occlusions. Despite using 18 cameras, there were a lot of occlusions for the markers fixed on the medial side of the limbs ($T_{2,4,18,20}$) or on the right side of the pelvis ($T_{8,10}$). The pelvis markers were also affected by the piked posture. This explained 21% of occlusions for the left anterior superior iliac spine marker T_7 . A general placement of cameras cannot solve the problem of occlusions since a specific placement for each athlete and each movement is needed. Many athletic movement analyses would be impaired if at least three markers were required to define each segment, because marker occlusions could not be avoided and marker interpolation for movements involving high acceleration can result in kinematics with large errors. This approach based on a chain model compensates for marker occlusion.

The reference kinematics was chosen as the result of the global optimisation with 16 markers (Kin_{16}) rather than the *direct approach* (Kadaba et al., 1990). In line with the works of Lu and O'Connor (1999) and Roux et al. (2002), global optimisation appears to be more accurate than the *direct approach*. While these studies were based on computer simulated trials, the noise added to the marker kinematics was systematic (Chèze et al., 1995), this being more appropriate to model skin movement artefacts than random noise as confirmed by Begon et al. (2007). Furthermore in the present study, the direct method could be applied for only a few frames due to the marker occlusions throughout the movement (Table 1). The global optimisation works with any prior defined kinematic model structure and any experimental movement data without any restriction on the marker number and location while the Hessian remains of full rank. The *HuMANs* toolbox (Wieber et al., 2006) allows new model chains to be implemented in order to reconstruct accurately the kinematics of movement with marker occlusions. The present algorithm will be improved in the future by introducing a weighting matrix in the Hessian and Jacobian expression and by a Kalman filter.

The precision of the kinematics obtained with the present algorithm was calculated for three sets of markers. The global error of reconstruction was about 27 mm for Kin_{16} and Kin_{11} . The global error increased to 31 mm for Kin_7 . The optimisation procedure always found a solution which depended on data accuracy and redundancy. Using redundant information (Kin_{16} and Kin_{11}), the chain model and markers compensated for each other's error. Since the error did not increase between Kin_{16} and Kin_{11} , the latter set of markers seemed to be a good compromise between the number of markers and their position to avoid skin movement artefacts. Global optimization provides a great opportunity to design optimal marker sets to minimize skin movement artefact, because less than three markers are needed on each body segment and the noisy markers can be removed.

The RMSDs found in this study for the thigh angles (q_{9-11}) could be discussed in line with the errors measured using intra-cortical pins (Reinschmidt et al., 1997a,b; Karlsson and Lundberg, 1994). In running (Reinschmidt et al., 1997b) the errors expressed as a percentage of the range of motion were 21% for flexion-extension, 64% for abduction-adduction and 70% for mediolateral rotation of the thigh. These RMSDs during the circling movement with Kin_{11} on high bar corresponded to 2%, 1% and 18% of the thigh ranges of motion. For Kin_7 , the RMSDs increased to 5%, 5% and 71%. Whatever the movement, the error associated with the mediolateral rotation of the thigh is the greatest. The study of Karlsson and Lundberg (1994) showed a difference of about 30° for the thigh mediolateral rotation calculated with skin-attached and bone-anchored markers (50° *versus* 20°). With global optimisation, the less noisy markers of pelvis and shank help to bring the thigh mediolateral rotation toward the correct orientation (Lu and O'Connor, 1999). The chain model and marker redundancy play an important role in compensating for errors. In this study, when the number of markers was reduced, the redundancy decreased and the inaccuracy increased. Since the knee was close to full extension, the mediolateral rotation (q_{11}) was poorly compensated for by the markers on the shank. The imprecision of q_{11} will have a small effect on the dynamics of straddled movements on high bar with straight legs. As the changes in knee flexion is small ($\Delta q_{12} \approx 10^\circ$) and as the knee should be fully extended in gymnastics, some assumptions could be introduced into the chain model for a reconstruction with seven markers. The thigh mediolateral rotation and knee flexion could be assumed to be zero throughout the movement. An alternative would be to express q_{11} as a function of thigh flexion-extension and abduction-adduction.

In conclusion, kinematics can be reconstructed with a chain model and a global optimisation procedure for a reduced number of markers. The chain model makes the most of the information contained in all the markers. In the case of circling movements on high bar with a piked straddled posture, 11 markers allowed a 12-*DoF* model to be reconstructed within a 3°, 4 mm error. With the modifications suggested above it should be possible to obtain good results with 7 markers. Future studies will be based on the simplification of the model by expressing the trunk flexion and the thigh mediolateral rotation as functions of thigh flexion-extension and abduction-adduction.

Conflict of interest statement

There are no conflicts of interest to declare by the authors.

Acknowledgements

The authors wish to acknowledge the support of the British Gymnastics World Class Programme and EGIDE (Ministère des Affaires Etrangères, France).

References

- Begon, M., Monnet, T., Lacouture, P., 2007. Effects of movement for estimating the hip joint centre. *Gait & Posture* 25, 353–359.
- Cappozzo, A., Catani, F., Leardini, A., Benedetti, M., Croce, U. D., 1996. Position and orientation in space of bones during movement: experimental artefacts. *Clinical Biomechanics* 11, 90–100.
- Challis, J. H., 1995. A procedure for determining rigid body transformation parameters. *Journal of Biomechanics* 28, 733–737.
- Charlton, I. W., Tate, P., Smyth, P., Roren, L., 2004. Repeatability of an optimised lower body model. *Gait & Posture* 20, 213–221.
- Chèze, L., Fregly, B. J., Dimnet, J., 1995. A solidification procedure to facilitate kinematic analyses based on video system data. *Journal of Biomechanics* 28, 879–884.
- Davis, R., Ounpuu, S., Tyburski, D., Gage, J., 1991. A gait analysis data collection and reduction technique. *Human Movement Science* 10, 575–587.
- Ehrig, R. M., Taylor, W. R., Duda, G. N., Heller, M. O., 2006. A survey of formal methods for determining the centre of rotation of ball joints. *Journal of Biomechanics* 39, 2798–2809.
- Hiley, M., Yeadon, M., 2003. Optimum technique for generating angular momentum in accelerated backward giant circles prior to a dismount. *Journal of Applied Biomechanics* 19, 119–130.
- Hiley, M., Yeadon, M., 2005. The margin for error when releasing the asymmetric bars for dismounts. *Journal of Applied Biomechanics* 21, 223–235.
- Kadaba, M., Ramakrishnan, H., Wootten, M., 1990. Measurement of lower extremity kinematics during level walking. *Journal of Orthopaedic Research* 8, 383–392.
- Karlsson, D., Lundberg, A., 1994. Accuracy estimation of kinematic data derived from bone anchored external markers. In *Proceedings of the 3rd International Symposium on 3-D Analysis of Human Motion*.
- Lu, T.-W., O'Connor, J., 1999. Bone position estimation from skin marker co-ordinates using global optimisation with joint constraints. *Journal of Biomechanics* 32, 129–134.
- Monnet, T., Desailly, E., Begon, M., Vallee, C., Lacouture, P., (in press) Comparison of the score and ha methods for locating in vivo the glenohumeral joint centre. *Journal of Biomechanics*.

- Reinbolt, J. A., Schutte, J. F., Fregly, B. J., Koh, B. I., Haftka, R. T., George, A. D., Mitchell, K. H., 2005. Determination of patient-specific multi-joint kinematic models through two-level optimization. *Journal of Biomechanics* 38, 621–626.
- Reinschmidt, C., Bogert, A., Lundberg, A., Nigg, B., Murphy, N., Stacoff, A., Stano, A., 1997a. Tibiofemoral and tibiocalcaneal motion during walking: external vs. skeletal markers. *Gait & Posture* 6, 98–109.
- Reinschmidt, C., Bogert, A., Nigg, B., Lundberg, A., Murphy, N., 1997b. Effect of skin movement on the analysis of skeletal knee joint motion during running. *Journal of Biomechanics* 30, 729–732.
- Roux, E., Bouilland, S., Godillon-Maquinghen, A.-P., Bouttens, D., 2002. Evaluation of the global optimisation method within the upper limb kinematics analysis. *Journal of Biomechanics* 35, 1279–1283.
- Spoor, C., Veldpaus, F., 1980. Rigid body motion calculated from spatial coordinates markers. *Journal of Biomechanics* 13, 391–393.
- Wieber, P.-B., Billet, F., Boissieux, L., Pissard-Gibollet, R., 2006. The humans toolbox, a homogeneous framework for motion capture, analysis and simulation. In: Ninth International Symposium on the 3D analysis of human movement.
- Yeadon, M. R., 1990. The simulation of aerial movement – II. A mathematical inertia model of the human body. *Journal of Biomechanics* 23, 67–74.